

## Supporting Information

---

### Formation of Ti-Fe mixed sulfide nanoboxes for enhanced electrocatalytic oxygen evolution

*Jianwei Nai,<sup>b</sup> Yan Lu,<sup>b</sup> and Xin-Yao Yu<sup>a\*</sup>*

<sup>a</sup>School of Materials Science and Engineering, Zhejiang University, Hangzhou 310027, P. R. China

<sup>b</sup>School of Chemical and Biomedical Engineering, Nanyang Technological University, 62 Nanyang Drive, Singapore 637459, Singapore

\* To whom all correspondence should be addressed. X.-Y. Y.: email, [yuxinyao@zju.edu.cn](mailto:yuxinyao@zju.edu.cn)

## Experimental Section

**Synthesis of Ti-Fe PBA nanocubes.** In a typical synthetic procedure, 75 mg of titanium(IV) fluoride and 3.0 g PVP (K30,  $M_w = 40,000$ ) were dissolved in 20 mL of HCl (0.1 M) solution under magnetic stirring for 1 h to form clear solution A. 253 mg of potassium hexacyanoferrate(II) trihydrate was dissolved in 20 mL of deionized (DI) water to form solution B. Then, solution B was added into solution A under magnetic stirring. After continuously stirring for 1 min, the obtained mixed solution was aged at 65 °C for 24 h. The precipitate was collected by centrifugation, washed with DI water and ethanol and dried at 70 °C overnight.

**Synthesis of Ti-Fe PBA nanoboxes.** In a typical synthetic procedure, 30 mg of Ti-Fe PBA nanocubes were dispersed in 30 mL of dimethylformamide (DMF) with assistance of ultrasonication for 15 min. Then the mixture was transferred into a 50 mL autoclave at 210 °C for 21 h in an electric oven. After the autoclave cooling down to room temperature, the precipitate was collected by centrifugation, washed with DI water and ethanol and dried at 70 °C overnight.

**Synthesis of crystalline Ti-Fe mixed sulfide nanoboxes (denoted as c-Ti-Fe-S boxes).** In a typical synthetic procedure, 10 mg of Ti-Fe PBA nanoboxes and 100 mg of thiourea powder were put at two separate positions in a porcelain boat with thiourea at the upstream side of the tube furnace. Then, the samples were annealed at 350 °C for 2 h with a heating rate of 2 °C  $\text{min}^{-1}$  under nitrogen atmosphere. The c-Ti-Fe-S boxes were obtained after cooling down to ambient temperature under nitrogen atmosphere.

**Synthesis of crystalline Ti-Fe mixed sulfide nanocubes (denoted as c-Ti-Fe-S cubes).** The synthetic procedure is similar with that for the c-Ti-Fe-S boxes, except using the Ti-Fe PBA nanocubes as the precursor for sulfuration.

**Synthesis of amorphous titanium sulfide mixed crystalline iron sulfide nanoboxes (denoted as a-Ti-S/c-Fe-S boxes).** The synthetic procedure is similar with that for the c-Ti-Fe-S boxes, except using 20 mg of the Ti-Fe PBA nanoboxes and 50 mg of sulfur powder as the S source for sulfuration.

**Synthesis of FeS<sub>2</sub> nanoparticles.** The Prussian blue (PB) nanoparticles were prepared first according to a previous report.<sup>1</sup> Then the sulfuration process is similar to that of the a-Ti-S/c-Fe-S boxes, which using sulfur powder as the S source.

**Materials characterization.** XRD patterns were collected on a Bruker D2 Phaser X-Ray Diffractometer with Ni-filtered Cu *K* $\alpha$  radiation ( $\lambda = 1.5406 \text{ \AA}$ ) at a voltage of 30 kV and a current of 10 mA. The morphology and structure of the products were characterized using FESEM (JEOL, JSM-6700F) equipped with EDX, and TEM (JEOL, JEM-1400/JEM-2010). The nitrogen adsorption measurement was carried out on Autosorb 6B at liquid-nitrogen temperature. X-ray photoelectron spectrometer (XPS, VG microtech ESCA2000) was used for the analysis of the composition of the as-synthesized samples.

**Electrochemical Measurements.** We first conducted a reversible hydrogen electrode (RHE) calibration. We used Pt sheet, Pt wire, and an Ag/AgCl electrode as the working electrode, counter electrode, and reference electrode, respectively. For all the electrochemical measurements, an aqueous solution of 1.0 M KOH was used as the electrolyte. Before calibration, the solution was bubbled with hydrogen for 0.5 h to get a hydrogen saturated electrolyte. Cyclic voltammetry (CV) was recorded at a scan rate of 2.0 mV s<sup>-1</sup> (Fig. S20). The average of the two potentials where the current crossed zero was taken to be the thermodynamic potential for the hydrogen electrode reactions. All the potentials shown in our tests were calibrated and transformed to RHE:  $E_{(\text{RHE})} =$

$E_{(\text{Ag}/\text{AgCl})} + 0.977 \text{ V}$ . To prepare the OER measurement, 2.0 mg of catalysts (for example, c-Ti-Fe-S boxes) was dispersed in 350  $\mu\text{L}$  of DI water, 135  $\mu\text{L}$  of ethanol and 15  $\mu\text{L}$  of 5 wt% Nafion solution to form a homogeneous ink. For fabrication of the working electrodes, 5  $\mu\text{L}$  of the catalyst ink was loaded onto a glassy carbon rotating disk electrode of 5 mm in diameter (loading amount was about 0.1  $\text{mg cm}^{-2}$ ). Then the electrode was dried at room temperature. The electrochemical studies were carried out in a standard three-electrode system using Pt wire and an Ag/AgCl electrode as the counter electrode and the reference electrode, respectively (controlled by a Pine Instruments electrochemistry workstation).  $\text{N}_2$  was used to purge the solution to achieve a  $\text{N}_2$ -saturated condition, while the working electrode was continuously rotated at 1600 rpm to get rid of the oxygen bubbles. Linear sweep voltammetry (LSV) was carried out at 5.0  $\text{mV s}^{-1}$  for the polarization curves. All polarization curves were corrected with  $iR$ -compensation. Electrochemical impedance spectroscopy (EIS) measurements were conducted in the range of 0.01 to  $10^5$  Hz with 0.01 V amplitude. The ECSA was estimated using the following method:  $i_c/(v \cdot C_s)$ , where  $i_c$  is the charging current,  $v$  is the scan rate and  $C_s$  is the specific capacitance of the sample which we take a general value of 0.040  $\text{mF cm}^{-2}$  in 1 M KOH.<sup>2</sup>

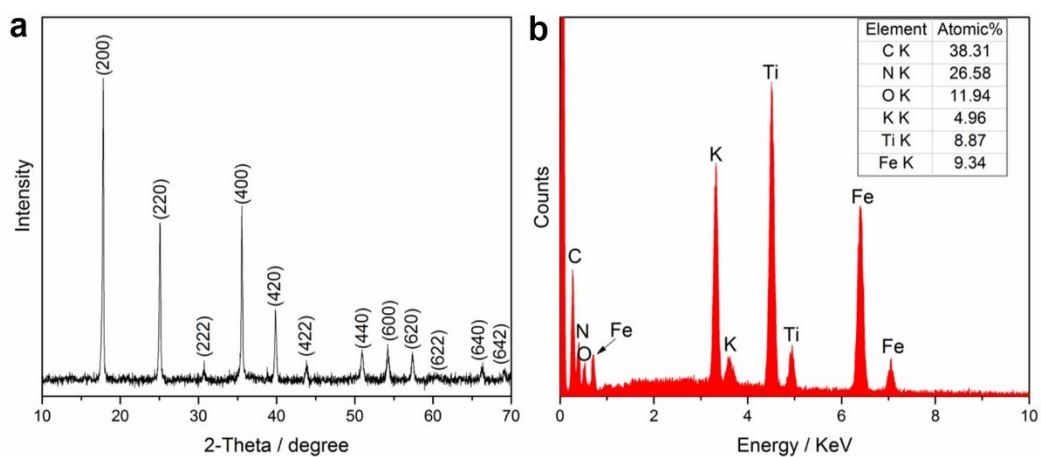


**Fig. S1** (a) XRD pattern and (b) EDX spectrum of the Ti-Fe PBA nanocubes. XRD result displays a typical pattern of the face-centered cubic structure of PBAs. EDX result indicates the atomic ratio of K/Ti/Fe is 0.53: 0.95: 1.

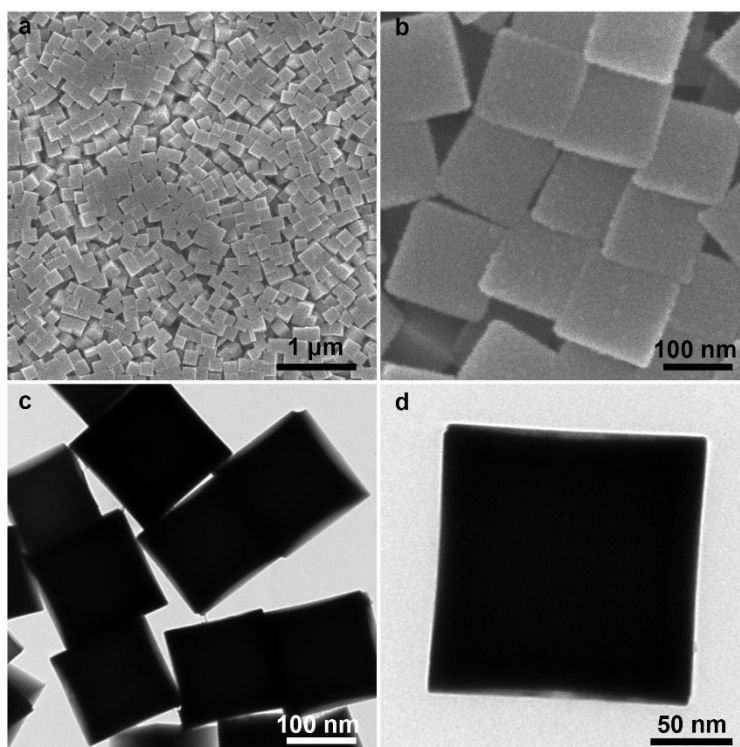


**Fig. S2** (a, b) SEM and (c, d) TEM images of the Ti-Fe PBA nanocubes.

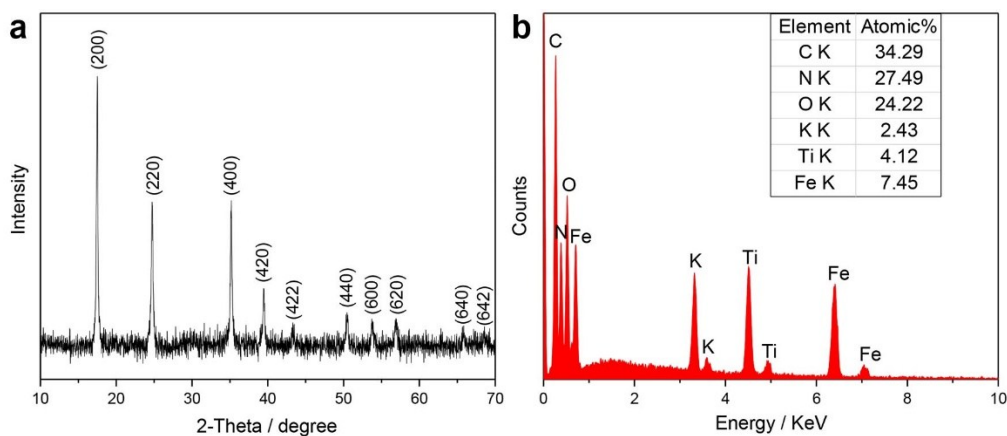


**Fig. S3** (a) XRD pattern and (b) EDX spectrum of the Ti-Fe PBA nanoboxes. XRD result displays a typical pattern of the face-centered cubic structure of PBAs. EDX result indicates the atomic ratio of K/Ti/Fe is 0.33: 0.55: 1.

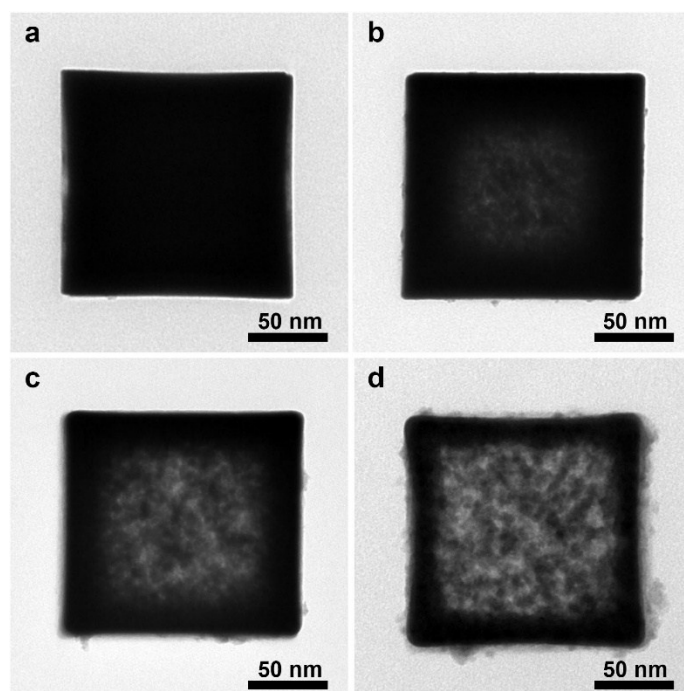


**Fig. S4** TEM images obtained from different stages at (a) 0, (b) 6, (c) 15, and (d) 21 h for the formation of nanoboxes, suggesting an inside-out hollowing mechanism due to a “soft” character of the center of the PBA nanocubes.

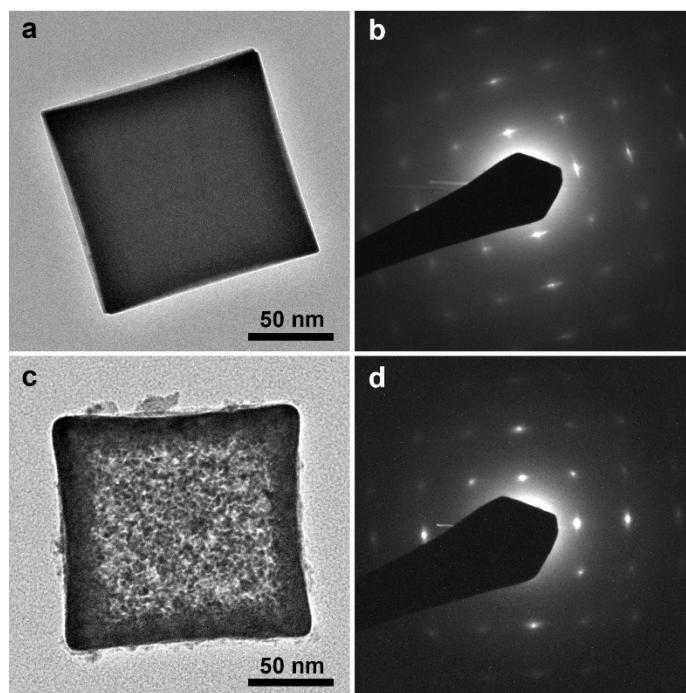


**Fig. S5** TEM images and SAED patterns of a typical Ti-Fe PBA (a, b) nanocube and (c, d) nanobox.

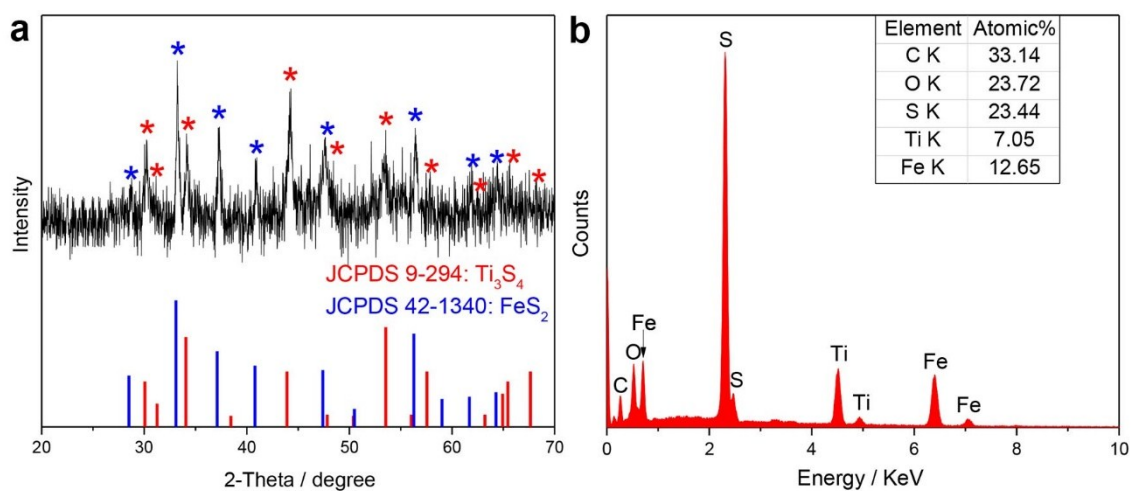


**Fig. S6** (a) XRD pattern and (b) EDX spectrum of the c-Ti-Fe-S boxes.

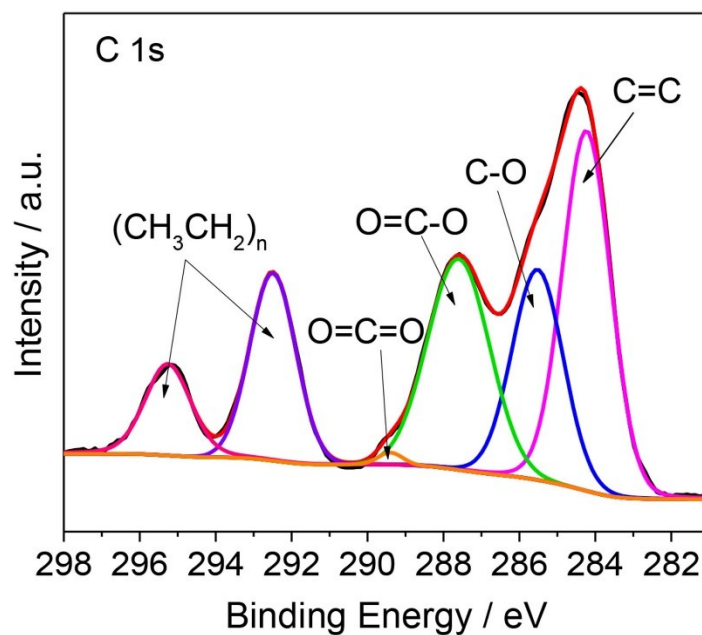


**Fig. S7** C 1s XPS spectrum of the c-Ti-Fe-S boxes. No C species can be assigned to carbides (binding energy is normally lower than 283 eV). Organic carbon compounds  $(\text{CH}_3\text{CH}_2)_n$  and amorphous carbon can be detected here, which might be formed by the reaction of cyano groups and hydrogen sulphide decomposed from the thiourea.

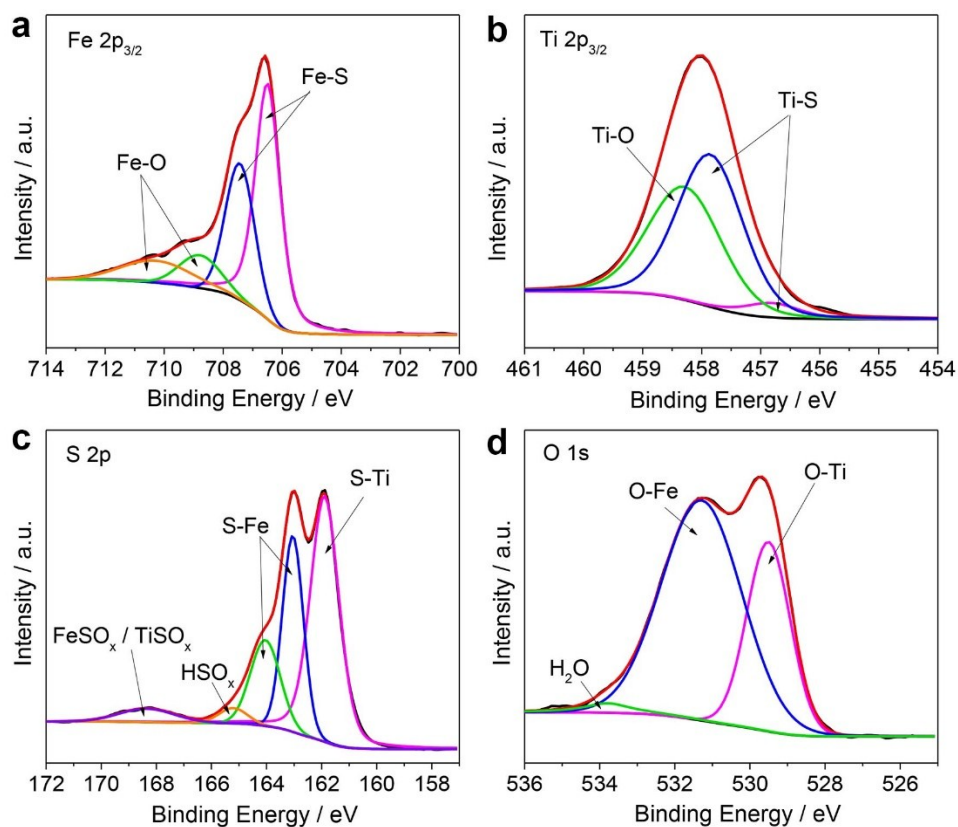


**Fig. S8** (a) Fe 2p<sub>3/2</sub>, (b) Ti 2p<sub>3/2</sub>, (c) S 2p and (d) O 1s XPS spectra of the as-prepared c-Ti-Fe-S boxes. From the Fe 2p<sub>3/2</sub> spectrum, the Fe<sup>2+</sup> and Fe<sup>3+</sup> can be detected. From the Ti 2p<sub>3/2</sub> spectrum, the Ti<sup>2+</sup> and Ti<sup>4+</sup> can be detected. All the four panels reveal a certain degree of oxidation on the surface of the c-Ti-Fe-S boxes.

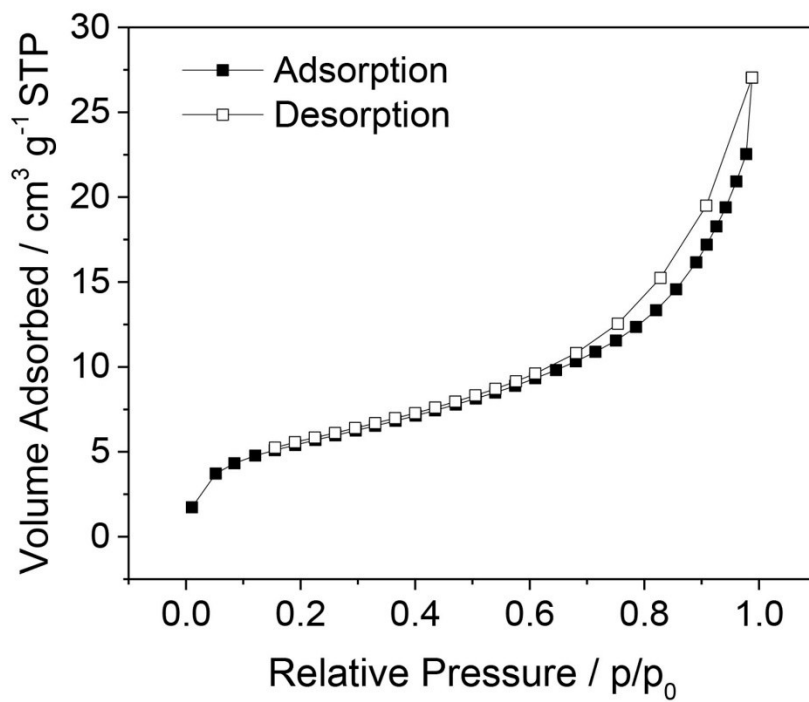


**Fig. S9** N<sub>2</sub> adsorption-desorption isotherm of the c-Ti-Fe-S boxes.

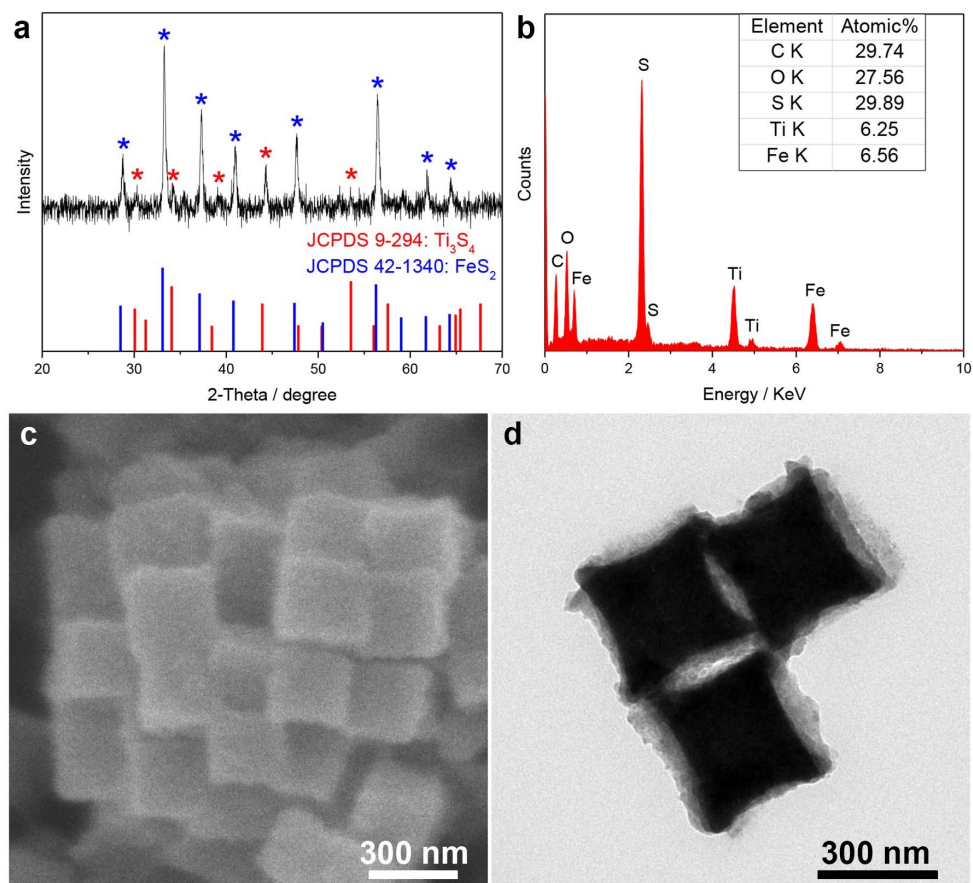


**Fig. S10** (a) XRD pattern, (b) EDX spectrum, (c) FESEM image, and (d) TEM image of the c-Ti-Fe-S cubes.

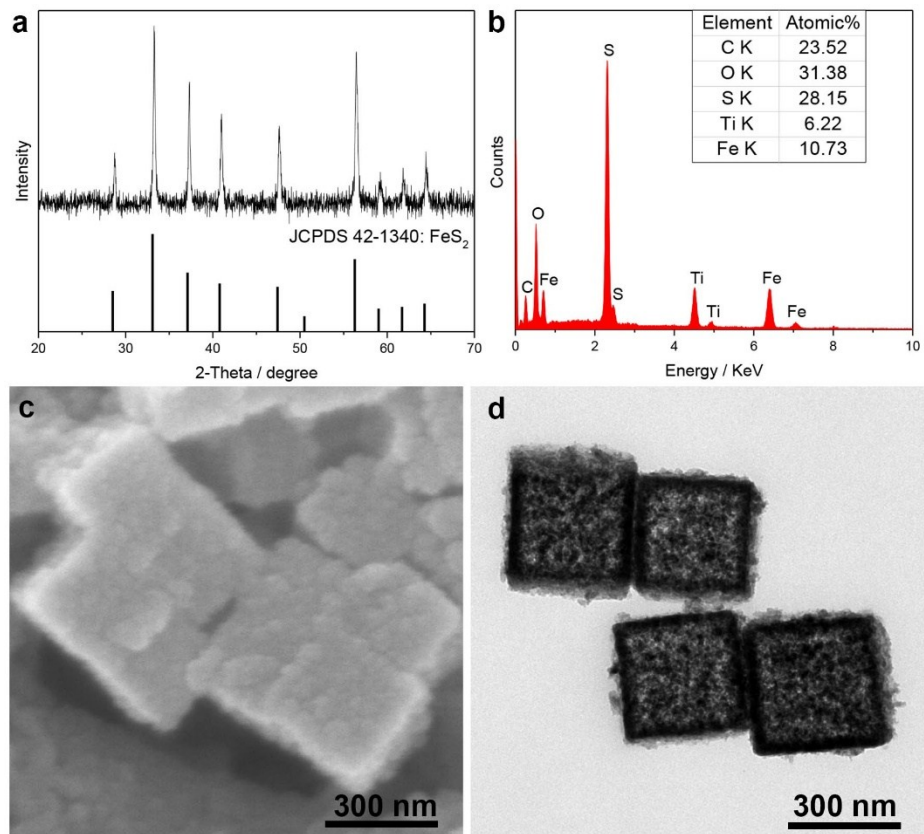


**Fig. S11** (a) XRD pattern, (b) EDX spectrum, (c) FESEM image and (d) TEM image of the a-Ti-S/c-Fe-S boxes.

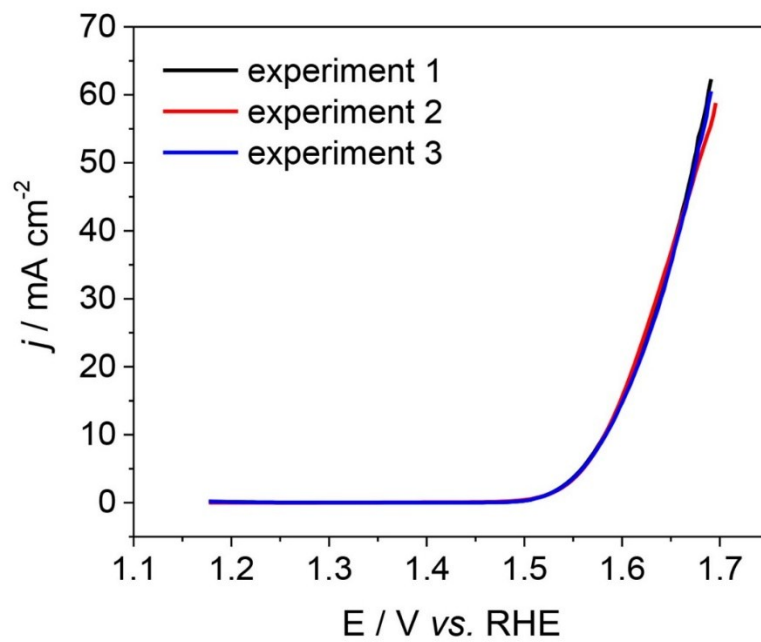


**Fig. S12** OER performance of the c-Ti-Fe-S catalyst from several experiments. The results show a good repeatability.

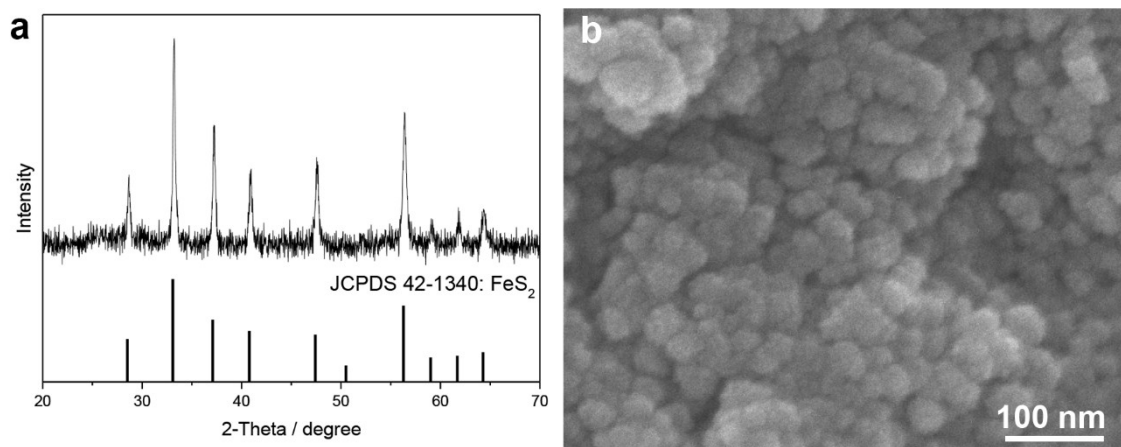


**Fig. S13** (a) XRD pattern and (b) FESEM image of the PB-derived FeS<sub>2</sub> nanoparticles.

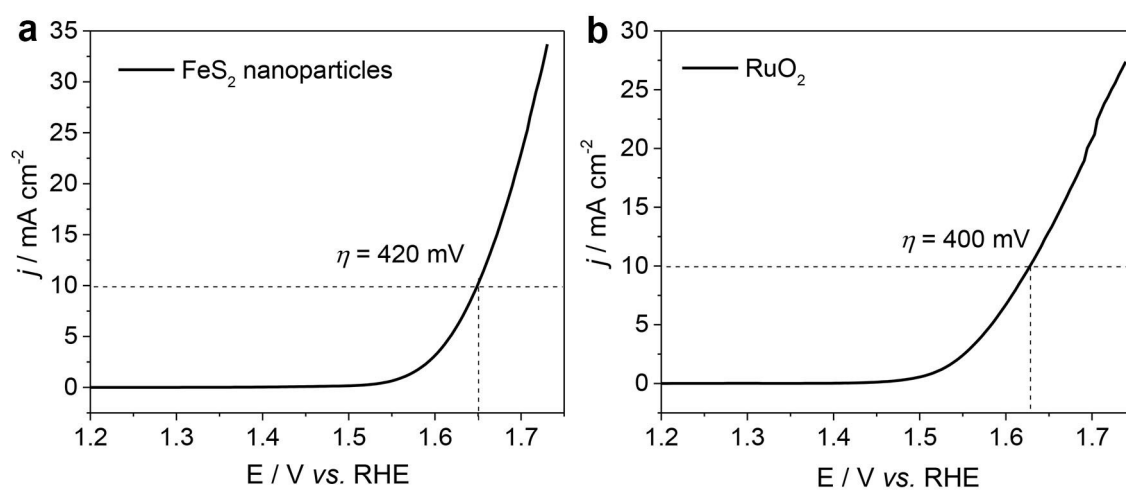


**Fig. S14** LSV curves of the (a) synthesized FeS<sub>2</sub> nanoparticles and (b) commercial RuO<sub>2</sub>.

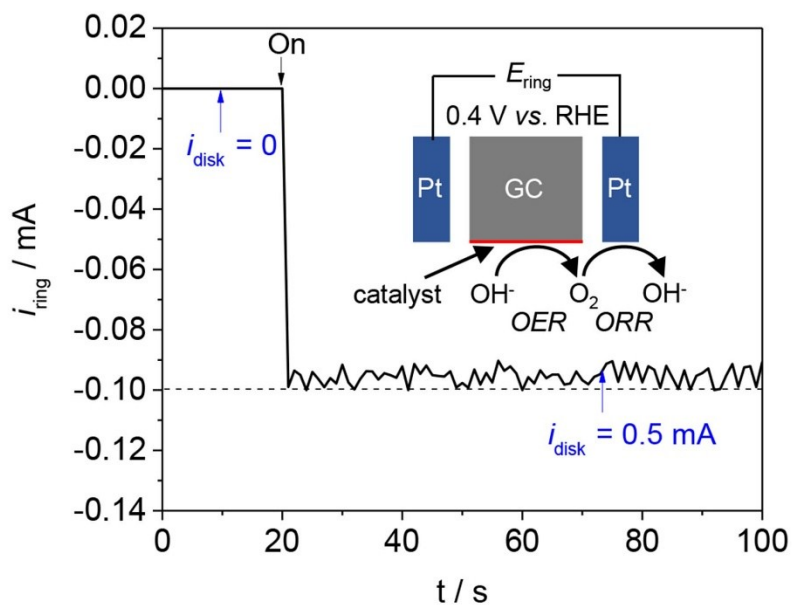


**Fig. S15** Ring currents when  $i_{\text{disk}}$  holds at 0 and 0.5 mA based on the RRDE technique of the c-Ti-Fe-S catalyst. The inset shows the schematic setting of the RRDE experiment: A ring potential of 0.40 V versus RHE is applied to detect the generated  $\text{O}_2$  molecules by the electrochemical oxygen reduction reaction (ORR), rendering a continuous OER (on glassy carbon disk electrode)  $\rightarrow$  ORR (on Pt ring electrode) process.

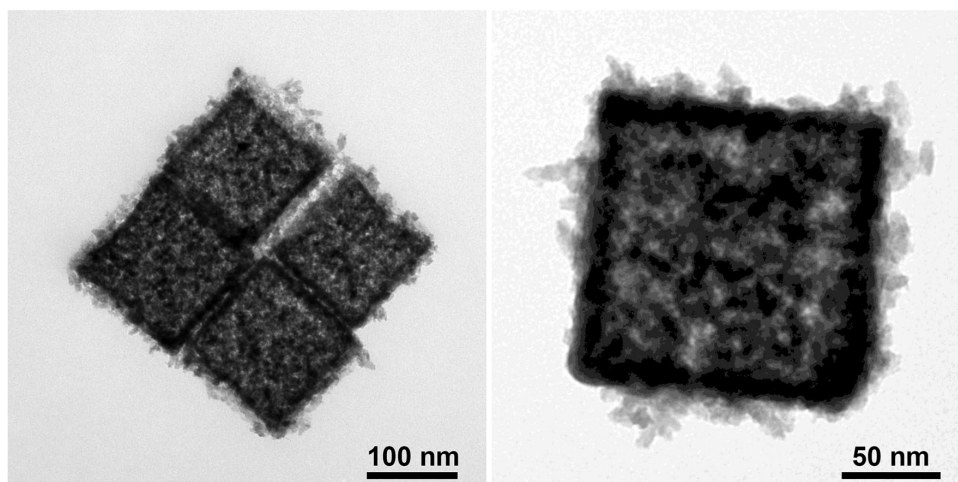


**Fig. S16** TEM images of the c-Ti-Fe-S boxes after the durability test.

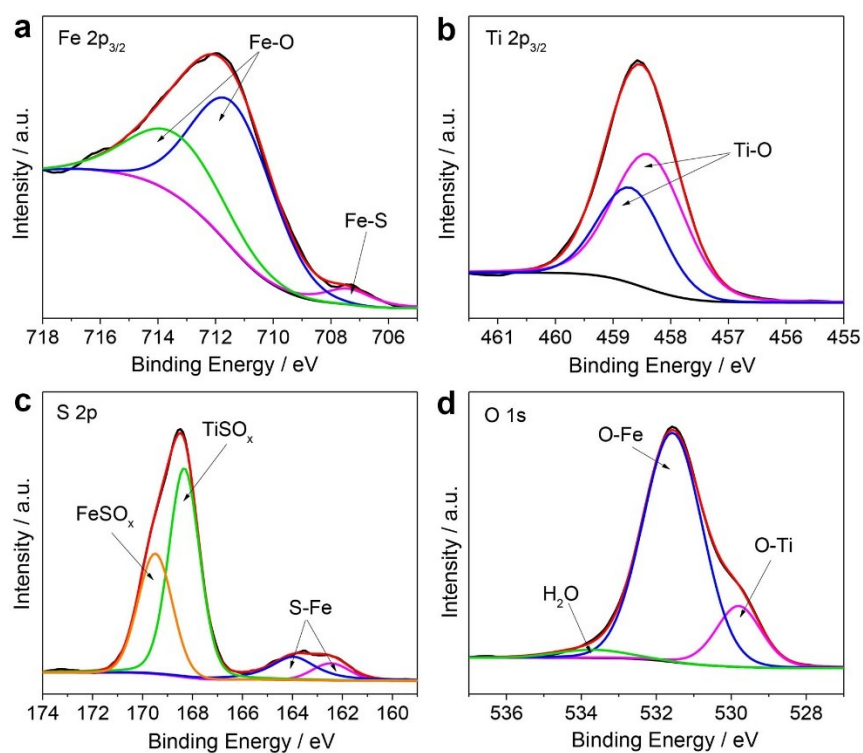


**Fig. S17** (a) Fe 2p<sub>3/2</sub>, (b) Ti 2p<sub>3/2</sub>, (c) S 2p and (d) O 1s XPS spectra of the c-Ti-Fe-S boxes after the durability test. All the four panels reveal a nearly complete transformation of sulfides to oxidized metal species on the surface of the c-Ti-Fe-S boxes.

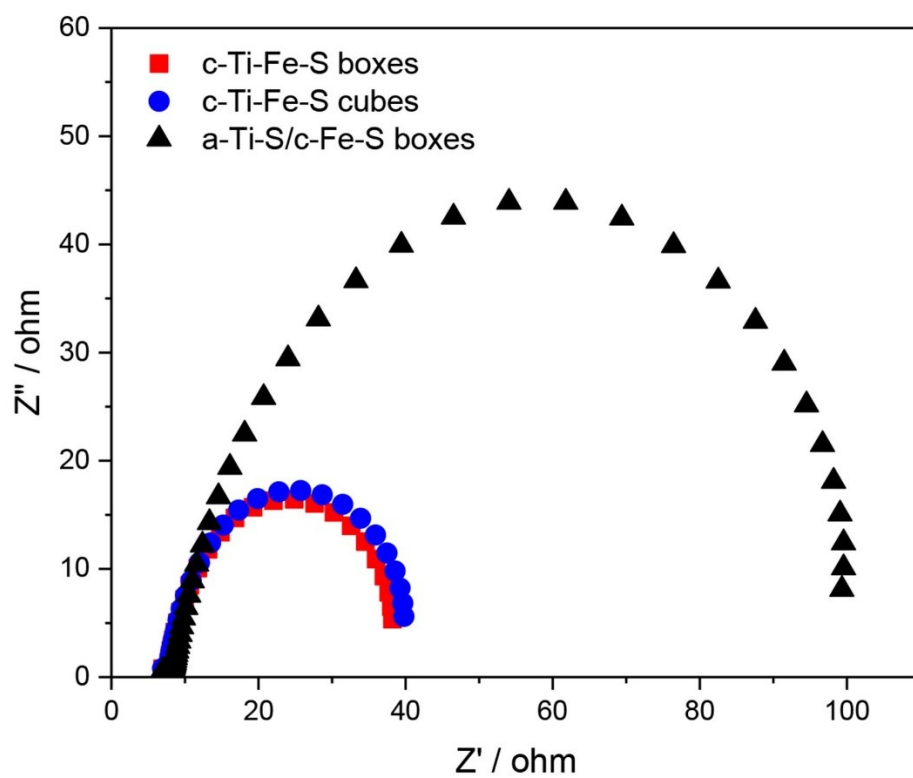


**Fig. S18** EIS plots of the catalysts.

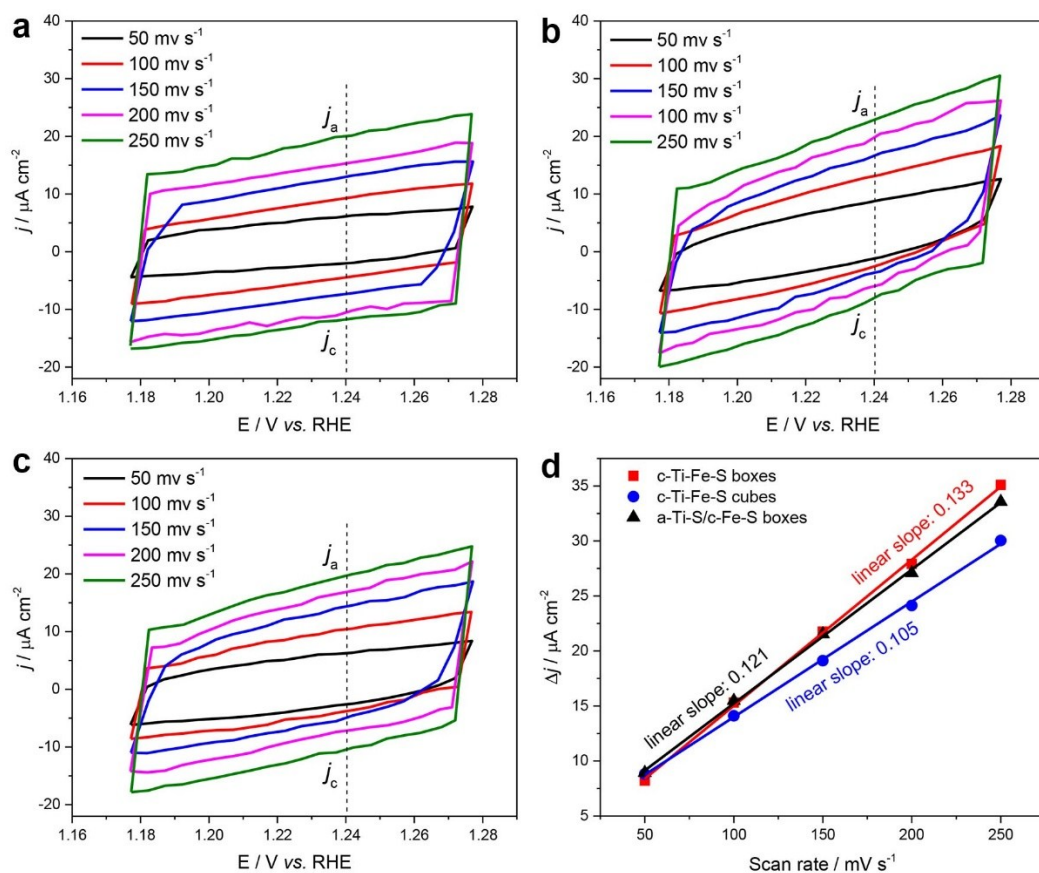


**Fig. S19** CV curves at different scan rates for the (a) c-Ti-Fe-S boxes, (b) c-Ti-Fe-S cubes, and (c) a-Ti-S/c-Fe-S boxes.  $j_a$  represents the anodic current density;  $j_c$  represents the cathodic current density.  $j_a$  and  $j_c$  taken at the potential of 1.24 V. (d) Current density ( $\Delta j = j_a - j_c$ ) as a function of scan rate derived from (a-c) for the three catalysts. The ECSA of the catalysts can then be estimated as  $0.33 \times 10^{-3}$ ,  $0.29 \times 10^{-3}$  and  $0.25 \times 10^{-3} \text{ cm}^2$  for the c-Ti-Fe-S boxes, a-Ti-S/c-Fe-S boxes and c-Ti-Fe-S cubes, respectively.

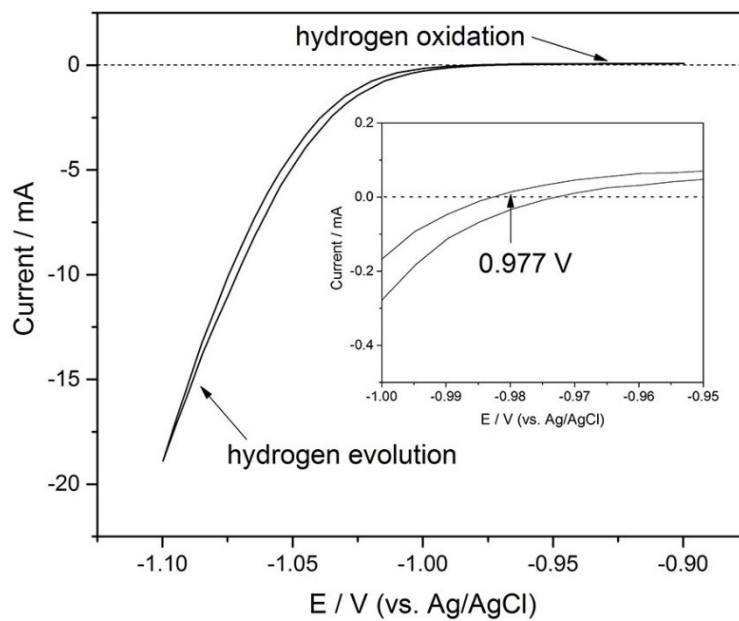


**Fig. S20** Reference electrode calibration in 1.0 M KOH solution.  $E_{(\text{RHE})} = E_{(\text{Ag/AgCl})} + 0.977$

V.

**Table S1.** Comparison of the OER activity (in 1.0 M KOH) of the c-Ti-Fe-S boxes prepared in this work with some recently reported catalysts.

<b>catalysts</b>	<b><math>\eta</math> (mV) at <math>j = 10 \text{ mA cm}^{-2}</math></b>	<b>Ref.</b>
c-Ti-Fe-S boxes	350	this work
NiCo <sub>2</sub> S <sub>4</sub> nanowire array/carbon cloth	340	3
NiCo <sub>2</sub> S <sub>4</sub> @N/S doped reduced graphene oxide	355	4
CoS <sub>2</sub> /N/S doped graphene oxide	370	5
atomic layer deposition NiS <sub>x</sub>	372	6
Co <sub>3</sub> S <sub>4</sub>	375	4
Ni <sub>3</sub> S <sub>2</sub> /Ni foam	410	7
carbon paper/carbon tubes/CoS	450	8
Ni <sub>3</sub> S <sub>4</sub>	555	4
Co <sub>3</sub> O <sub>4</sub> microframes	370	9
Co-Fe mixed oxide nanoframes	350	10
Ni-Co mixed oxides nanocages	360	11
Mesoporous Cu <sub>x</sub> Co <sub>y</sub> O <sub>4</sub>	390	12
Co <sub>3</sub> O <sub>4</sub> /graphene hybrid	310	13
Zn <sub>x</sub> Co <sub>3-x</sub> O <sub>4</sub> nanoarrays	320	14
Fe <sub>3</sub> C in porous graphite	299	15
Fe/Fe <sub>3</sub> C	505	16
Co <sub>4</sub> Mo <sub>2</sub> @N-doped carbon	330	17

## References

- 1 D. Cai, B. Liu, D. Wang, L. Wang, Y. Liu, B. Qu, X. Duan, Q. Li and T. Wang, *J. Mater. Chem. A*, 2016, **4**, 183.
- 2 C. C. L. McCrory, S. Jung, J. C. Peters and T. F. Jaramillo, *J. Am. Chem. Soc.*, 2013, **135**, 16977.
- 3 D. Liu, Q. Lu, Y. Luo, X. Sun and A. M. Asiri, *Nanoscale*, 2015, **7**, 15122.
- 4 Q. Liu, J. Jin and J. Zhang, *ACS Appl. Mater. Interfaces*, 2013, **5**, 5002.
- 5 P. Ganesan, M. Prabu, J. Sanetuntikul and S. Shanmugam, *ACS Catal.*, 2015, **5**, 3625.
- 6 H. Li, Y. Shao, Y. Su, Y. Gao and X. Wang, *Chem. Mater.*, 2016, **28**, 1155.
- 7 C. Ouyang, X. Wang, C. Wang, X. Zhang, J. Wu, Z. Ma, S. Dou and S. Wang, *Electrochim. Acta*, 2015, **174**, 297.
- 8 J. Wang, H.-X. Zhong, Z.-L. Wang, F.-L. Meng and X.-B. Zhang, *ACS Nano*, 2016, **10**, 2342.
- 9 Y. Feng, X.-Y. Yu and U. Paik, *Chem. Commun.*, 2016, **52**, 6269.
- 10 J. Nai, B. Y. Guan, L. Yu and X. W. Lou, *Sci. Adv.*, 2017, **3**, e1700732.
- 11 L. Han, X.-Y. Yu and X. W. Lou, *Adv. Mater.*, 2016, **28**, 4601.
- 12 T. Grewe, X. Deng, C. Weidenthaler, F. Schüth and H. Tüysüz, *Chem. Mater.*, 2013, **25**, 4926.
- 13 Y. Liang, Y. Li, H. Wang, J. Zhou, J. Wang, T. Regier and H. Dai, *Nat. Mater.*, 2011, **10**, 780.
- 14 X. Liu, Z. Chang, L. Luo, T. Xu, X. Lei, J. Liu and X. Sun, *Chem. Mater.*, 2014, **26**, 1889.
- 15 Y. Zhang, J. Zai, K. He and X. Qian, *Chem. Commun.*, 2018, **54**, 3158.

16 B. K. Barman and K. K. Nanda, *Green Chem.*, 2016, **18**, 427.

17 J. Jiang, Q. Liu, C. Zeng and L. Ai, *J. Mater. Chem. A*, 2017, **5**, 16929.